

Accepted version on Author's Personal Website: C. R. Koch

Article Name with DOI link to Final Published Version complete citation:

David Gordon, Christian Wouters, Shota Kinoshita, Maximilian Wick, Bastian Lehrheuer, Jakob Andert, Stefan Pischinger, and Charles R Koch. Homogeneous charge compression ignition combustion stability improvement using a rapid ignition system. *International Journal of Engine Research*, 21(10):1846–1856, 2020. doi: [10.1177/1468087420917769](https://doi.org/10.1177/1468087420917769)

See also:

https://sites.ualberta.ca/~ckoch/open_access/IJER_Rapid_Ign_DG_2020.pdf

Post-print

As per publisher copyright is ©2020



This work is licensed under a
[Creative Commons Attribution-NonCommercial-NoDerivatives 4.0 International License](https://creativecommons.org/licenses/by-nc-nd/4.0/).



Article accepted version starts on the next page →

[Or link: to Author's Website](#)

Homogeneous charge compression ignition combustion stability improvement using a rapid ignition system

International J of Engine Research

2020, Vol. 21(10) 1846–1856

© IMechE 2020

Article reuse guidelines:

sagepub.com/journals-permissions

DOI: 10.1177/1468087420917769

journals.sagepub.com/home/ijer



David Gordon¹ , Christian Wouters² , Shota Kinoshita³,
Maximilian Wick⁴, Bastian Lehrheuer², Jakob Andert⁵ ,
Stefan Pischinger² and Charles R Koch¹

Abstract

When compared to traditional engines, homogeneous charge compression ignition has the potential to significantly reduce NO_x raw emissions, while maintaining a high fuel efficiency. Homogeneous charge compression ignition is characterized by compression-induced autoignition of a lean homogeneous air–fuel mixture. Since homogeneous charge compression ignition does not utilize direct ignition control, it is strongly dependent on the state of the cylinder charge and can suffer from high cyclic variability. With spark-assisted compression ignition, it has been demonstrated that misfires can be reduced, while preserving the high thermal efficiency of homogeneous charge compression ignition as a result of the more favorable physical mixture properties due to dilution. However, spark-assisted compression ignition reduces the NO_x benefits of homogeneous charge compression ignition, as it increases the local combustion temperatures. To merge the advantages of the homogeneous charge compression ignition and the spark-assisted compression ignition combustion processes, a field-programmable gate array for detailed simulation of the physical gas exchange is combined with a rapid spark system. The low latency and computational speed of the field-programmable gate array allows the simulation process to be implemented in real time. When combined with the rapid reaction time of the high-frequency current-based rapid ignition system, a feedforward controller based on the cylinder pressure or heat release is realized. The developed model-based controller determines if a spark is required to assist the homogeneous charge compression ignition combustion process. The use of the field-programmable gate array and rapid ignition system allows for the calculation of combustion properties and controller output within 0.1 °CA. This article presents the development and experimental validation of the developed controller on a single-cylinder research engine. The combustion stability has been significantly improved as reflected in an improved standard deviation of the indicated mean effective pressure and a reduction of the combustion phasing variations. Furthermore, compared to a traditional homogeneous charge compression ignition system, the hydrocarbon emissions can be reduced, while maintaining low NO_x emissions.

Keywords

Field-programmable gate array, homogeneous charge compression ignition, gasoline-controlled autoignition, gas exchange model, zero-dimensional engine simulation, model-based control, rapid ignition system, spark-assisted compression ignition

Date received: 17 October 2019; accepted: 13 February 2020

Introduction

Homogeneous charge compression ignition (HCCI) is a part-load combustion method, which is characterized by lean low-temperature combustion (LTC) with temperatures below the oxides of nitrogen (NO_x) formation temperature of 2000 K. As a result, HCCI has the potential to significantly reduce NO_x emissions, while maintaining a high fuel efficiency, comparable with

¹Department of Mechanical Engineering, University of Alberta, Edmonton, AB, Canada

²Institute for Combustion Engines, RWTH Aachen University, Aachen, Germany

³SOOKEN, INC., Research division 1, Research department 12, Tokyo, Japan

⁴FEV Europe GmbH, Aachen, Germany

⁵Mechatronics Systems for Combustion Engines, RWTH Aachen University, Aachen, Germany

Corresponding author:

David Gordon, Department of Mechanical Engineering, University of Alberta, 116 Street & 85 Avenue, Edmonton, AB T6G 2R3, Canada.

Email: dgordon@ualberta.ca

current stratified lean-burn combustion, with NO_x emissions reduced by up to 99%.^{1–3} Therefore, expensive exhaust aftertreatment systems can be reduced or simplified.⁴ Efficiency also improves when using HCCI combustion due to the rapid global and spatial combustion in combination with reduced wall heat losses from the LTC. The potential of HCCI combustion has been proven in numerous research projects.^{5,6}

HCCI combustion is enabled by compression-induced autoignition, which is highly dependent on the cylinder state during compression. The lack of a direct combustion timing control method like ignition timing in spark ignition (SI) engines or injection timing in traditional compression ignition (CI) engines is a major disadvantage, which has caused a strong research focus on control strategies.^{7–9}

Near the misfire limit, when using exhaust gas recirculation (EGR) as a means to provide the thermal energy required to achieve autoignition, a strong coupling between cycles can exist.¹⁰ As dilution is increased, a reduction in the rate of combustion reactions leads to increased chances for quenching and flameout.¹¹ This leads to increased fuel transfer through EGR and a bifurcated engine operating condition as the combustion transitions between stable and unstable combustion modes. This bifurcated behavior leads to a transition from a low indicated mean effective pressure (IMEP) cycle to a high IMEP cycle.¹² Multi-cycle computational fluid dynamics (CFD) models have also been used to show this effect and have determined that the remaining fuel and intermediate species from the previous cycle can lead to combustion during the negative valve overlap (NVO) recompression and an early combustion phasing in the following cycle.¹³

Consequently at lean operating conditions, the tendency for unstable combustion sequences increases, which proves to be problematic especially during engine transients and near the misfire limit. Current cycle-based control strategies only stabilize a small portion of the operation range, which is insufficient for practical engine deployment.¹⁴ Therefore, a stabilizing controller which works over a wide range of operating conditions is needed. Distinct cyclic variations, characterized by a spontaneous shift from stable to unstable operation, have been investigated in literature.^{15–17} Various control interactions have been explored to reduce this cyclic coupling and extend the HCCI operating range but with varying success.^{18,19}

One of the main challenges with HCCI is the increased unburnt hydrocarbon (uHC) and carbon monoxide (CO) emissions which are the result of lower combustion temperatures and complete or partial misfires where little or no fuel is burnt. This limitation of HCCI can be reduced by the addition of a supporting spark; however, this supporting spark increases the local combustion temperature causing an increase in NO_x emissions. The combination of SI leading to HCCI autoignition in the end-gas is referred to as spark-assisted compression ignition (SACI) which

provides the ability to extend the load range of HCCI. However, the use of SACI leads to reduced combustion stability at the lean operation limit compared to HCCI.^{20–22} Currently, SACI is also a very active area of research as researchers explore the influence of spark timings and intake heating on combustion stability.²³

In this work, a rapid ignition system (RIS) will be controlled using a real-time gas exchange model running on a field-programmable gate array (FPGA) to provide a spark only on cycles with late combustion phasing. The model is able to calculate the cylinder state within 0.1 crank angle degrees ($^\circ\text{CA}$), and using the RIS, a spark can be introduced within 5–10 μs to help prevent misfire cycles while limiting the number of cycles which require spark and increase NO_x .

Experimental setup

A single-cylinder research engine (SCRE) outfitted with a fully variable electro-magnetic valve train (EMVT) is used to validate the online FPGA gas exchange model. The EMVT is controlled using the FPGA board which is part of the engine control unit (ECU). The flexibility of the valve timing allows for engine operation with combustion chamber exhaust gas recirculation through NVO. This allows for a wide operating range of HCCI combustion timings. The fuel injector is a piezoelectric outward-opening hollow cone injector that is controlled using the FPGA. The fuel used for all testing in this work is conventional European Research Octane Number (RON) 96 gasoline containing 10% ethanol. Engine geometry and testing conditions are listed in Table 1. Two operating points (OPs), OP A and OP B, are used in this work. These engine OPs are listed in Table 2. OP A will be used for all development work, and then the controllers will be tested at the lower load OP B.

The in-cylinder pressure is measured using a Kistler A6061B piezoelectric pressure transducer. The intake and exhaust manifold pressures are measured using

Table 1. Single-cylinder research engine parameters.

Parameter	Value
Displacement volume	0.499 L
Stroke	90 mm
Bore	84 mm
Compression ratio	12:1
No. of valves (In/Ex)	2/2
Valve train	EMVT
Max. valve lift (In/Ex)	8 mm/8 mm
Valve angle (In/Ex)	22.5°/22.5°
Valve diameter (In/Ex)	32 mm/26 mm
Intake air pressure	1013 mbar
Exhaust pressure	1013 mbar
Oil and coolant temperature	90 $^\circ\text{C}$
Engine speed	1500 r/min
Fuel rail pressure	100 bar

EMVT: electro-magnetic valve train.

Table 2. Engine operating conditions.

Operating point	A	B
IMEP (bar)	4.0	2.7
EVO ($^{\circ}$ CA aTDC)	180	160
EVC ($^{\circ}$ CA aTDC)	293.5	282
IVO ($^{\circ}$ CA aTDC)	426.5	438
IVC ($^{\circ}$ CA aTDC)	545	545
Intake temperature ($^{\circ}$ C)	75	60
EOI_{main} ($^{\circ}$ CA aTDC)	448	448
$m_{inj,main}$ (mg)	11.8	8.1
λ (-)	1.4	1.5

IMEP: indicated mean effective pressure; EVO: exhaust valve opening; EVC: exhaust valve closing; IVO: intake valve opening; IVC: intake valve closing; CA: crank angle; aTDC: after top dead center.

Kistler 4045-A5 piezoresistive pressure transducers. Kistler charge amplifiers are used to output the measured pressure as a voltage. The position of the electromagnetic valves is measured using FEV conductive lift measurement sensors, while the position of the crank is measured using a hall effect encoder.

An FEV combustion analysis system (CAS) is used to record cylinder pressure at a 0.1° CA resolution for use in the offline detailed model. The pressure signals are simultaneously input to the FPGA board contained in the prototyping ECU. Details of the MicroAutoBox II (MABX) prototyping ECU are provided in Gordon et al.²⁴

The RIS is designed for providing the ability to have a spark begin immediately after the ignition trigger signal is received. To achieve such a fast response, a high-frequency current system is utilized. Traditional ignition systems utilize stored magnetic energy by charging a coil which is used to provide a spark between the gap of the plug. However, these conventional ignition systems require significant charging time (typically 3–10 ms) when compared to the desired control action speed needed here. In the RIS, the high-frequency current supplied to the primary coil from the power supply unit generates an alternating magnetic field, and the field yields alternating high voltage on the secondary coil immediately. Thus, the RIS does not require charging time, allowing for the spark to begin within approximately 5–10 μ s, which is approximately 1000 times shorter than that of conventional systems. The RIS has sufficient bandwidth for the proposed control strategy.

Control strategy and motivation

To improve HCCI combustion stability, large cyclic variations need to be reduced. One metric to represent variation of combustion is the combustion phasing represented by the crank angle where 50% of the heat from combustion has been released also known as CA_{50} . Figure 1 shows the experimentally measured cylinder pressure signal of three consecutive cycles. Cycle 1 is typical of a standard cycle with a CA_{50} of 12

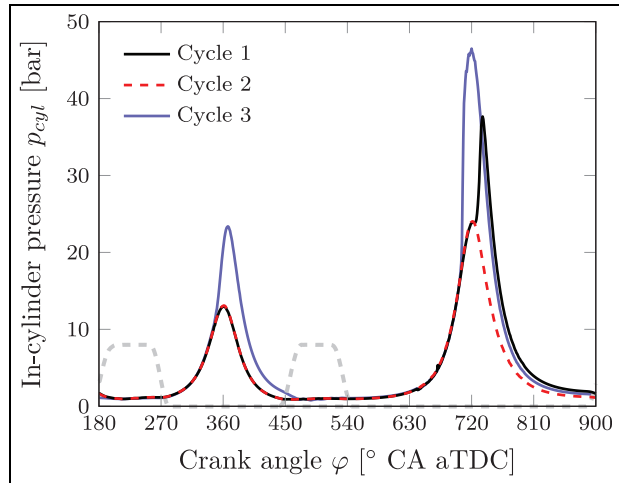


Figure 1. Distinct cyclic variation in the in-cylinder pressure p_{cyl} trace at operating point A.²⁸

$^{\circ}$ CA after top dead center (aTDC). It is then followed by cycle 2 which can be considered an incomplete combustion with a very late combustion phasing. Then, due to the incomplete combustion, residual fuel is transferred to the next cycle (cycle 3) through internal EGR. As the combustion phasing is very late in cycle 2, the in-cylinder temperature increases which subsequently increases the temperature of the exhaust gas transferred to cycle 3. There is also the possibility that during the NVO recompression a portion of the residual fuel ignites (as seen in cycle 3) and leads to a further temperature increase in the residual exhaust gas. In addition, the combustion during the NVO recompression increased the pre-reactions leading to an increase in H_2O_2 formation. This increase in temperature and combustion radicals leads to an early combustion phasing with a high pressure rise rate. An early combustion phasing is not desired as the high pressure rise rate leads to increased combustion noise and possible engine damage.^{25,26} Overall, high cyclic variation of combustion also tends to reduce thermal efficiency and increase exhaust emissions.²⁷

Figure 2 shows the return map for the combustion phasing, CA_{50} . A return map is used to show the relationship between the combustion phasing of the current cycle, $CA_{50}(i)$, and of the following one, $CA_{50}(i + 1)$. In stable operation, two consecutive cycles are not correlated, so the return map would show random scatter around the combustion phasing mean. The spread of the data points represents the stochastic variation from cycle to cycle.¹⁰ However, when a distinct pattern or branching can be seen on the return map as is the case in Figure 2, a direct coupling between cycles exists. To effectively stabilize combustion, the spread of the data points and distinct “V” should be reduced.

In previous work, the cyclic variation of HCCI has been reduced by preventing the early combustion following a misfire (cycle 3 in Figure 1) using direct water

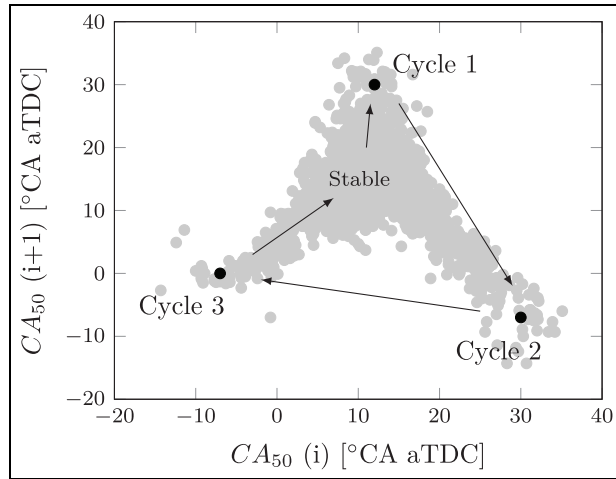


Figure 2. Distinct cyclic variation in the corresponding combustion phasing CA_{50} return map at operating point A.²⁸

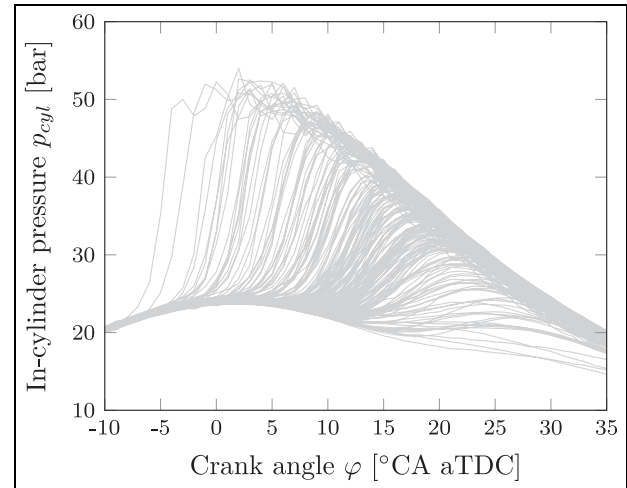


Figure 3. Cyclic variability in the cylinder pressure during HCCI combustion at operating point A.

injection to cool the trapped exhaust gas to retard combustion phasing back to the desired value.^{28–30} However, that leaves cycle 2 unaffected and the engine experiences a misfire leading to higher emissions and lower efficiency. The use of water injection adds the requirement for a second injection system and the requirement for a high quality water source for implementation in production vehicles.³¹ To prevent a complete misfire, the use of a spark interaction during cycle 2 in Figure 1 is presented in this work. This supporting spark will be used only when necessary to help preserve the NO_x benefits of HCCI combustion by keeping the combustion temperature low.

Pressure-based control strategy

The high cyclic variability of HCCI combustion can be seen when examining the range of in-cylinder pressure of 200 cycles at a specified crank angle as seen in Figure 3. In this figure, the motoring pressure (cylinder pressure without combustion) can be seen where all the cycles overlap when late combustion occurs. This difference in measured cylinder pressure compared to the baseline motoring pressure provides a method to determine if auto ignition has started.

The large variation in cylinder pressure presented in Figure 3 shows that at a given crank angle there is a large variation in cylinder pressure. By selecting a specific CA and then examining the correlation of the in-cylinder pressure with the combustion phasing of that cycle results in Figure 4. When considering the correlation between cylinder pressure and the combustion phasing of that cycle at an engine angle before TDC (-10 or -5 °CA aTDC), it is very difficult to observe anything other than cycles with very early combustion phasings. This is not useful for spark control as we are trying to distinguish late cycles from early ones. However, when considering the cylinder pressure after

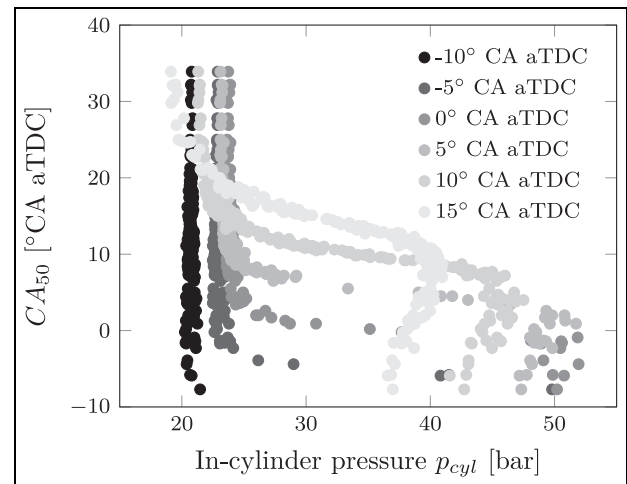


Figure 4. Correlation between upcoming combustion phasing and cylinder pressure at a specified crank angle aTDC, operating point A.

0 °CA aTDC, a clear correlation of the combustion phasing with the cylinder pressure is observed. This requirement to examine cylinder pressure at 0 °CA limits the controller calculation time since effective actuation needs to occur as early as possible. At 5 °CA aTDC, a clear distinction between cycles with a combustion phasing later than 10 °CA aTDC can be made. These cycles, later than 10 °CA aTDC, are considered to have a late combustion phasing and will require support with a spark.

At 5 °CA aTDC, if the cylinder pressure has not exceeded the motoring pressure (23.5 bar for the engine used) plus 10%, it is assumed that the combustion will be late or a misfire is going to occur and a spark is required. There will be some cycles when the spark will be activated even though the ignition timing is only slightly retarded at around 12 °CA aTDC; however, it

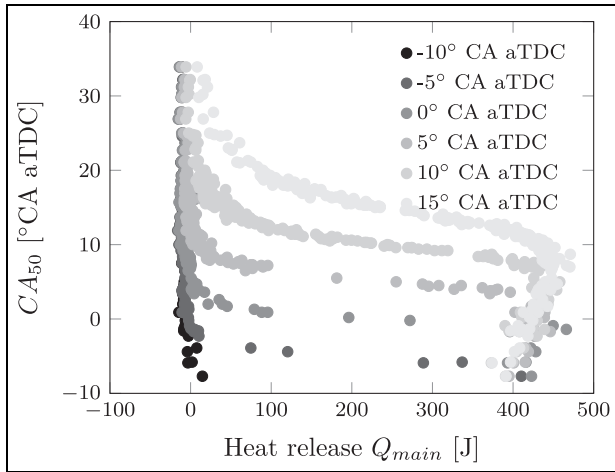


Figure 5. Correlation between upcoming combustion phasing and cumulative heat release at a specified angle aTDC, operating point A.

is important to keep the spark as early as possible to ensure it has enough time for the flame to propagate through the fuel/air mixture.

As the threshold is based on motoring pressure, it would need to be recalculated based on the physical dimensions of the engine in use. This is not the case with the heat release-based control strategy presented in the following section.

Heat release-based control strategy

The increase in cylinder pressure is due to the start of the combustion process, which can also be shown using the accumulated heat release. The advantage of using heat release over just measured cylinder pressure is that a very large change in value is observed at the start of the combustion process. Therefore, the effect of signal noise can be reduced.

The heat released from the combustion process is calculated using the specific heat ratio $\gamma(\phi)$, the actual cylinder volume $V(\phi)$ and the cylinder pressure $p(\phi)$, all as a function of crank angle ϕ , the heat release, $dQ_b/d\phi$, is calculated as

$$\frac{dQ_b}{d\phi} = -\frac{1}{\gamma-1} V \frac{dp}{d\phi} - \frac{\gamma}{\gamma-1} p \frac{dV}{d\phi} + \frac{dQ_w}{d\phi} \quad (1)$$

The heat transfer $dQ_w/d\phi$ of the cylinder charge to the walls is calculated using the Hohenberg equation.³² This real-time gas exchange model is described in detail in Gordon et al.²⁴

Figure 5 shows a similar result to the pressure-based correlation (Figure 4) when the heat release at a specified angle aTDC is correlated to the combustion phasing of that cycle.

As in the pressure correlation, 5 °CA aTDC is selected as the timing when to monitor if combustion has begun. If not, the SI system is activated. Figure 6

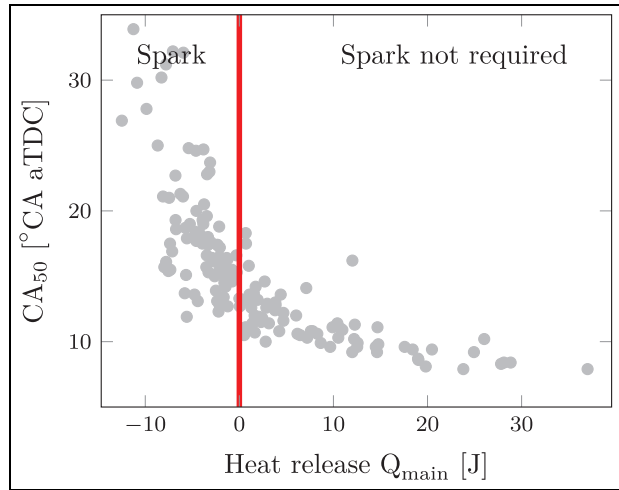


Figure 6. Selected threshold for start of combustion using correlation between upcoming combustion phasing and cumulative heat release at 5 °CA aTDC, operating point A.

shows the correlation for only 5 °CA aTDC and just the transition area around 0 J heat release. In this case, a heat release threshold of 0 J is selected as a physical representation of the start of combustion. This threshold predicts the combustion phasing will be approximately 15 °CA aTDC or later.

Ignition timing constraints

The above two control strategies are then implemented on the FPGA side of the engine controller as shown schematically in Figure 7. The proposed feedforward control strategy takes the cylinder pressure or cumulative heat release at an engine angle of 5 °CA aTDC and compares it to the specified threshold (discussed in the previous section). If it is determined that the combustion has yet to begin, the RIS is sent a signal for the spark to begin.

With HCCI combustion, the cylinder state is very close to the auto ignition point of the fuel and air mixture even in cases of late combustion or misfire. Therefore, only a small amount of additional energy is required for the auto ignition process to begin. However, after the piston reaches TDC, the expanding cylinder volume lowers the cylinder pressure and increases the amount of additional energy required for combustion to begin. Therefore, it is desirable to have the spark occur as early as possible.

Another advantage of using the FPGA is the computation speed for in-cycle control. Using the rapid calculation rate of the FPGA allows for the calculation of the entire gas exchange process including heat release using the existing model.²⁴ The gas exchange process is calculated on the FPGA every 0.1 °CA which provides the heat release rate in 3.5250 μs.²⁴ Therefore, the engine can be operated up to 4728 r/min before the resolution of the heat release rate cannot be maintained

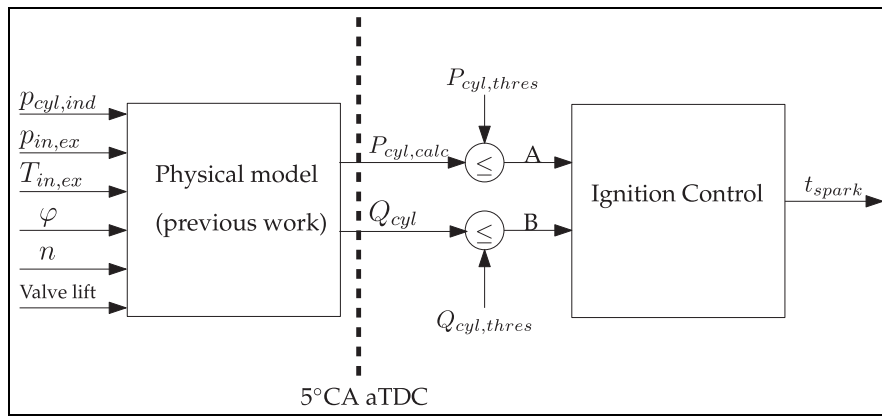


Figure 7. Feedforward spark control structure.

within 0.1 °CA. As HCCI is a low-mid speed combustion method that is generally limited to around 3000 r/min, the proposed control strategy can be applied to the entire HCCI operating range.⁸

The calculation of the controller output is completed with a delay of only 301 FPGA samples (or 3.76 μ s for the FPGA used in this study). When combined with the high speed of the RIS ignition system, the spark begins in 5–10 μ s (0.045–0.09 °CA at 1500 L/min) after the engine reaches 5 °CA aTDC. Therefore, when using an FPGA-based model and RIS system, the spark can occur when the cylinder state is close to auto ignition and provide the maximum time for the fuel to burn before the exhaust valve opens. Using the proposed control strategy with traditional ignition systems (which require around 3–10 ms for coil charging) would significantly reduce the amount of time for the fuel to burn as shown in Figure 8.

When using a FPGA, the total physical resources are limited. Therefore, when additional controllers are implemented, it is important to determine the additional amount of resources utilized. When compared to the existing gas exchange model running on the FPGA,²⁴ the proposed controller consumes under 1% of the available flip-flops and look-up tables on the Xilinx FPGA used.

Combustion stability

The proposed feedforward controller was tested using both the in-cylinder pressure and heat release as control input on the SCRE with the goal of reducing the cyclic variation shown in Figure 1. The performance of the heat release-based controller at stabilizing the combustion phasing can be seen in Figure 9. Here, 1000 consecutive cycles are presented with the controller being activated after 500 cycles. The variation in combustion phasing after cycle 500 is significantly reduced after the controller is enabled as shown by the reduction in standard deviation from 6.89 to 5.3 °CA or a reduction of 23%.

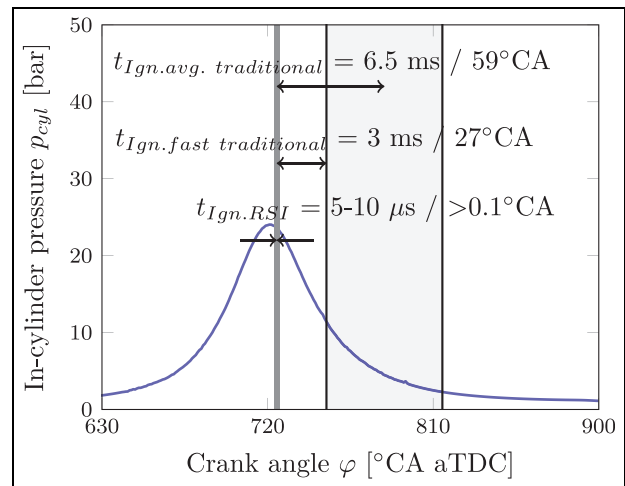


Figure 8. Ignition discharge time based on control signal at 5 °CA aTDC and operating point A. Gray area represents variation in traditional ignition systems.

Before the controller is activated, there are eight cycles with a combustion phasing later than 30 °CA aTDC (considered a misfire). After the controller is activated, there are no cycles with a combustion phasing greater than 30 °CA aTDC, showing the controller is able to completely eliminate misfire cycles for this case. After the controller is enabled, the most retarded combustion phasing is now 27.4 °CA aTDC which occurs on cycle 516. This means that after the spark is fired at 5 °CA aTDC it takes 22 °CA for 50% of the fuel to burn. This is still a long delay and highlights the importance of having the spark as early as possible.

Figure 9 also shows that the number of early combustion phasing cycles has been greatly reduced even though the spark does not have a direct effect on these cycles. This reduction in cycles with a very advanced combustion phasing is due to the fuel being burnt in the desired cycle instead of being transferred to subsequent cycles. This shows that the proposed control method is

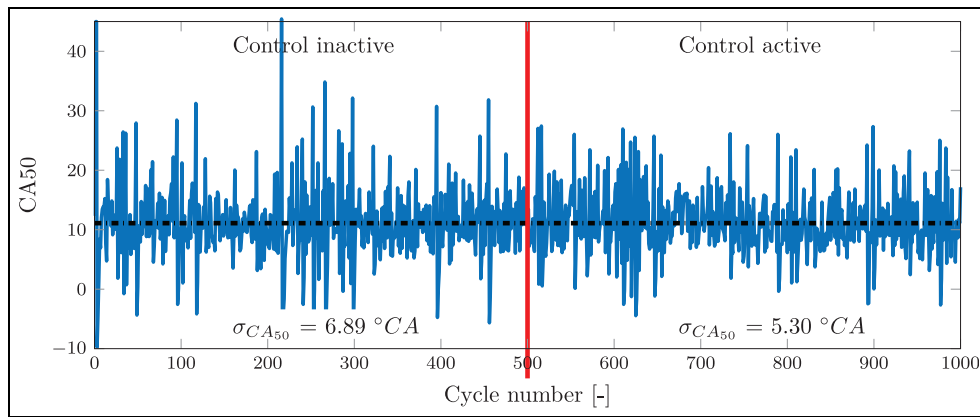


Figure 9. Combustion phasing, CA_{50} , stability improvement with in-cycle controller based on heat release at $5^{\circ}CA$ aTDC. The controller is activated after 500 cycles, operating point A.

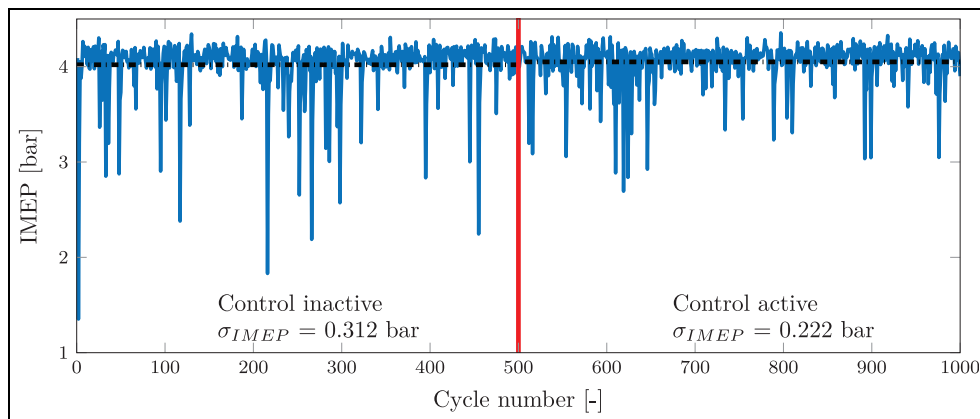


Figure 10. IMEP stability improvement with in-cycle controller based on heat release at $5^{\circ}CA$ aTDC. The controller is activated after 500 cycles, operating point A.

able to significantly reduce coupling between subsequent cycles.

A similar improvement due to the proposed controller can be seen when examining the torque produced each cycle as shown by the change in IMEP presented in Figure 10. With the spark controller deactivated, there are 13 cycles with an IMEP below 3 bar and 6 cycles with an IMEP below 2.5 bar representing cycles with a very late and inefficient combustion. With the spark controller activated, there are only four cycles with an IMEP below 3 bar and no cycles with an IMEP below 2.5 bar. This improvement can also be seen as the reduction of the standard deviation of IMEP from 0.312 to 0.222 bar with the controller activated, which represents a 28.9% reduction in the standard deviation of IMEP showing a significant improvement in the combustion stability of HCCI.

The controller's ability to decouple subsequent cycles can be seen in the return map shown in Figure 11. When the controller is inactive (red squares), the

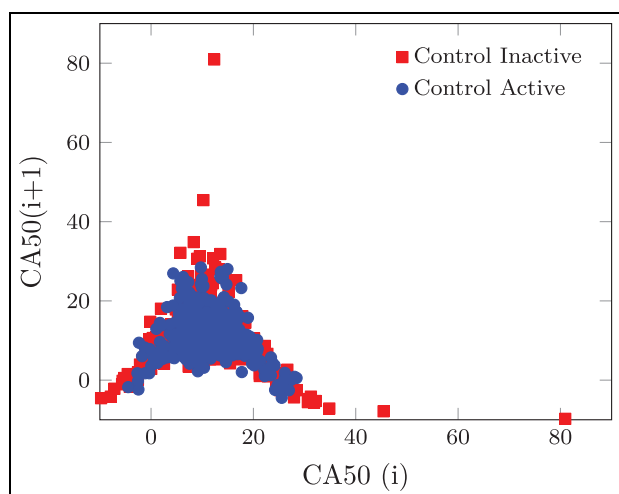


Figure 11. Effect of tested controller on the combustion phasing return map, operating point A.

Table 3. Combustion stability improvement due to feedforward rapid spark controller. Control input of cylinder pressure (pres) and heat release (HR) are both shown.

Control input Controller	Operating point	IMEP (bar)		CA ₅₀ (°CA)		$\Delta\sigma_{IMEP}$ (%)	$\Delta\sigma$ CA ₅₀ (%)	$\overline{\Delta dp/d\phi}$ (%)	Control interactions (cycles)
		Off	On	Off	On				
Pres	B	2.86	2.89	9.4	9.6	−21.2	−12.9	−1.0	117/500
Pres	A	4.03	4.04	11.0	11.1	−13.8	−2.5	−1.4	25/500
HR	B	2.71	2.72	9.4	9.4	−5.0	−1.9	−1.6	71/500
HR	A	3.92	3.96	11.0	10.8	−25.2	−34.3	−0.8	121/500
HR	A	4.02	4.05	11.1	11.1	−28.9	−23.0	−1.9	86/500

IMEP: indicated mean effective pressure; CA: crank angle.

characteristic “V” shaped spread of data presented in Figure 2 is observed. When the controller is activated (round blue data points), there is reduction of the data points in the arms of the return map and the distinct shape is reduced down with shorter arms. This demonstrates that the developed controller is successful in reducing the cycles with an extremely retarded combustion phasing which then prevents cycles with a very advanced combustion phasing.

Table 3 presents a summary of the two tested control strategies at two OPs. The two OPs have varied loads at 3- and 4-bar IMEP. At both of the OPs, the controller showed an increase in the average IMEP when the controller is activated. This shows that the control strategy is able to improve the combustion efficiency by delivering more power out of the same fuel. There is very little change in the average combustion phasing which is expected as the controller is preventing both very retarded and advanced combustion phasing cycles. Therefore, there is almost no change of the average combustion phasing which is desired.

The standard deviation of both IMEP and combustion phasing is significantly reduced when the controller is activated. This large reduction shows that the controller is successfully able to stabilize HCCI combustion which helps to provide a smoother running engine. The reduction in peak pressure rise rate is also shown in Table 3. While this improvement is relatively small, the proposed controller does not directly reduce the pressure rise rate and all the reduction seen is due to improved combustion stability.

As load is changed, the same thresholds designed for 4-bar IMEP above are used for the lower load (3-bar IMEP) for both the pressure and heat release-based control strategies. By changing load, the right hand side of Figures 4 and 5 would change due to changes in the peak pressure and total heat release. However, the left hand side of the curves in the Figures would remain unchanged as this is due to the motoring pressure and minimum heat release. This is beneficial as our control strategy is looking at catching cycles not exceeding the motoring pressure or minimum heat release and this is unaffected by the changes in load. The motoring pressure (or cylinder pressure during fired operation) will change due to varying the engine speed (at constant

load) only due to varying wall heat losses based on the time scale. The resulting differences in pressure can however be neglected for this control system/application, and it is expected that the proposed controller would also handle changes in engine speed.

As both control methods perform similarly, it is recommended that the heat release method be used as it does not need to be calibrated to the motoring pressure like the pressure-based controller. Thus, it can be applied to various engines while reducing the calibration effort.

Emission benefits

With the addition of a spark to an HCCI engine, the improvement in combustion stability is expected. However, the NO_x benefits of HCCI occur due to the rapid multi-site LTC which is reduced when a spark is used to initiate the combustion process. When a spark is introduced to start the combustion process, the spark creates a single point of ignition that propagates through the cylinder and increases the local gas temperature to above the NO_x formation temperature.

The proposed control strategy is aimed at reducing the uHC emissions related to misfire by providing a spark to help the combustion process begin, while preserving the benefit of not having a spark when not needed. The proposed ignition control strategy was compared with the cases of no spark interaction (HCCI) and having a spark every cycle at 5 °CA aTDC (SACI). For each ignition strategy, three measurements were performed with each measurement consisting of averaging the emission measurement over 30 s.

Figure 12 shows that the expected increase NO_x and NO emission was observed when the spark was always used. The nitrogen oxide emissions remain constant between the pure HCCI case and the controller operation. This result is expected as the spark is only used in approximately 10% of cycles. Even in the 1 in 10 cycles the spark is used, the combustion occurs very late and as the cylinder volume is increasing which helps to keep the combustion temperature below the NO_x formation temperature.

The uHC emissions produced when compared to the two reference cases can be seen in Figure 13. When the

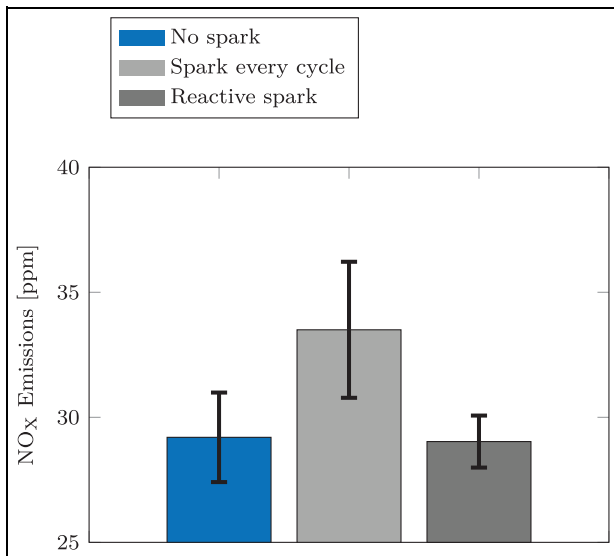


Figure 12. Comparison of nitrogen oxide emissions between control strategies.

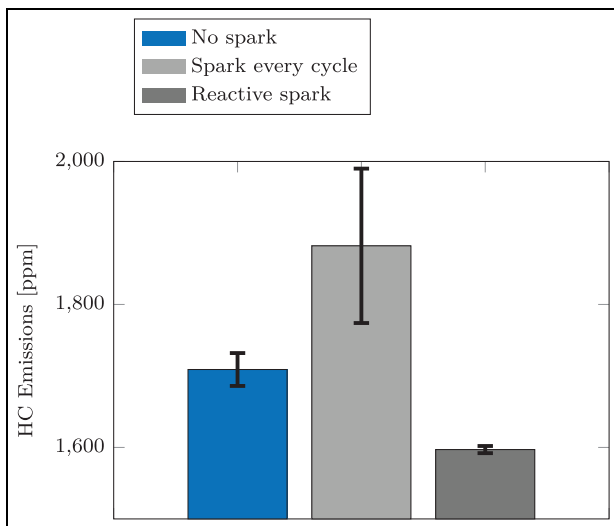


Figure 13. Comparison of unburnt hydrocarbon emissions between control strategies.

controller is enabled, we see the lowest hydrocarbon (HC) emissions over both reference points. Then compared to the pure HCCI case (no spark), an improvement of 6.6% is achieved. However, the case where the spark occurs, every cycle actually has the highest HC emissions. When a spark is always used, it is expected that a hotter more complete combustion occurs every cycle; however, the very late spark timing leads to SACI combustion which experiences a very high cyclic variability at very late spark timings.^{21,22} This high cyclic variability leads to unstable combustion and increased HC emissions. Similarly, the carbon monoxide emissions are also increased in the SACI case as seen in Figure 14 which matches the HC emission results.

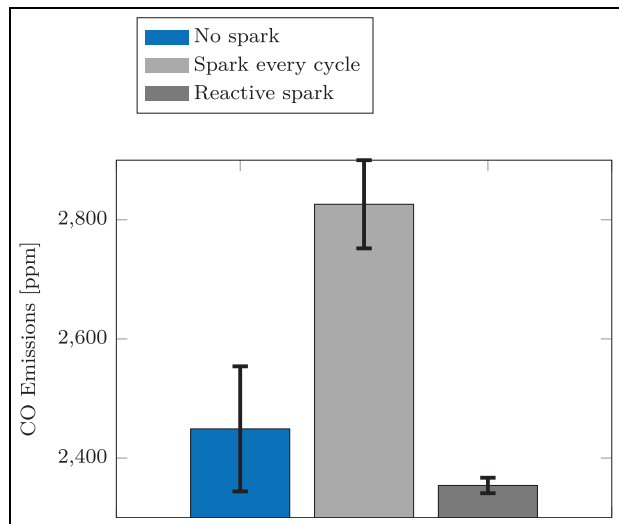


Figure 14. Comparison of carbon monoxide emissions between control strategies.

The high cyclic variability of the SACI case as seen by the large standard deviation of the emissions is presented. When the spark was used in every cycle, the combustion stability is decreased compared to the pure HCCI operating condition. This decrease in combustion stability is due to an increase in the amount of fuel burnt using flame propagation compared to the auto-ignition of HCCI. The large standard deviation is also due to the limited number of tests performed; however, the basic benefit of the proposed control strategy is shown. To better understand the impact to the engine emission output, further research is needed to allow for a larger data set.

Conclusion and future work

The RIS was combined with the fast calculation rate of an FPGA-based engine controller to experimentally test an ignition controller. This controller utilizes either the cylinder pressure or heat release to determine if the auto ignition process of HCCI has started. The proposed controller was able to successfully reduce the standard deviation of combustion phasing and IMEP at multiple OPs. The controller required a spark in approximately 10% of cycles at the OP tested. This led to nitrogen oxide levels similar to the pure HCCI case while showing an improvement of 6.6% in uHC emission over pure HCCI.

The tests performed showed the potential of the controller to improve HCCI combustion stability; however, to fully understand the emission benefits, further testing is required to statistically evaluate the emission improvement of the proposed controller. The ignition controller was able to successfully reduce the number of misfire cycles. Combining this controller with direct water injection to help control the thermal energy transferred between cycles could further improve the

HCCI combustion stability and is the focus of our future work.





Declaration of conflicting interests

The author(s) declared no potential conflicts of interest with respect to the research, authorship, and/or publication of this article.

Funding

The author(s) disclosed receipt of the following financial support for the research, authorship, and/or publication of this article: This work was performed as part of the research group 2401, funded by DFG (Deutsche Forschungsgemeinschaft) and Future Energy Systems at the University of Alberta. In addition, the authors acknowledge the support of the Natural Sciences and Engineering Research Council of Canada (NSERC). The RIS is provided by the DENSO Corporation and their support is also gratefully acknowledged.

ORCID iDs

David Gordon  <https://orcid.org/0000-0002-7999-8234>
 Christian Wouters  <https://orcid.org/0000-0002-2562-3146>
 Jakob Andert  <https://orcid.org/0000-0002-6754-1907>
 Charles R Koch  <https://orcid.org/0000-0002-6094-5933>

References

- Breitbach H, Waltner A, Landefeld T and Schwarz C. Lean-burn stratified combustion at gasoline engines. *MTZ Worldwide* 2013; 74(5): 10–16.
- Langen P, Melcher T, Missy S, Schwarz C and und Schünemann E Neue BMW sechs- und vierzylinder-ottomotoren mit high precision injection und schichtbrennverfahren. In: 28. Internationales Wiener Motorensymposium, 26–27 April 2007. Vienna, Austria: VDI-Verlag.
- Reitz RD, Ogawa H, Payri R, Fansler T, Kokjohn S, Moriyoshi Y, et al. IJER editorial: The future of the internal combustion engine. *Int J Eng Res* 2020; 21(1): 3–10.
- Zhao H. *HCCI and CAI engines for the automotive industry*. Boca Raton, FL: Woodhead Publishing, 2007.
- Brassat A. *Betriebsstrategien der kontrollierten Selbstzündung am aufgeladenen direkteinspritzenden Ottomotor*. PhD Dissertation, RWTH Aachen University, Aachen, 2013.
- Ebrahimi K. *Model based control of combustion timing and load in HCCI engines*. PhD Dissertation, University of Alberta, Edmonton, AB, Canada, 2016.
- Ritter D, Andert J, Abel D and Albin T. Model-based control of gasoline-controlled auto-ignition. *Int J Eng Res* 2018; 19(2): 189–201.
- Andert J, Wick M, Lehrheuer B, Sohn C, Albin T and Pischinger S. Autoregressive modeling of cycle-to-cycle correlations in homogeneous charge compression ignition combustion. *Int J Eng Res* 2018; 19(7): 790–802.
- Vaughan A. *Adaptive machine learning for modeling and control of non-stationary, near chaotic combustion in real-time*. PhD Dissertation, The University of Michigan, Ann Arbor, MI, 2015.
- Ghazimirsaeid A and Koch CR. Controlling cyclic combustion timing variations using a symbol-statistics predictive approach in an HCCI engine. *Appl Energy* 2012; 92: 133–146.
- CE Finney, BC Kaul, CS Daw, RM Wagner, KD Edwards, B Johnney, et al. Invited review: a review of deterministic effects in cyclic variability of internal combustion engines. *Int J Eng Res* 2015; 16(3): 366–378.
- Hunicz J. Cycle-by-cycle variations in autonomous and spark assisted homogeneous charge compression ignition combustion of stoichiometric air–fuel mixture. *Int J Spray Combust Dynam* 2018; 10(3): 231–243.
- Shingne PS. *Thermodynamic modeling of HCCI combustion with recompression and direct injection*. PhD Dissertation, The University of Michigan, Ann Arbor, MI, 2015.
- Saxena S and Bedoya ID. Fundamental phenomena affecting low temperature combustion and HCCI engines, high load limits and strategies for extending these limits. *Prog Energy Combust Sci* 2013; 39(5): 457–488.
- Hellstrom E, Larimore J, Jade S, Stefanopoulou AG and Jiang L. Reducing cyclic variability while regulating combustion phasing in a four-cylinder HCCI engine. *IEEE T Control Syst Tech* 2014; 22(3): 1190–1197.
- Larimore J. *Experimental analysis and control of recompression homogeneous charge compression ignition combustion at the high cyclic variability limit*. PhD Dissertation, The University of Michigan, Ann Arbor, MI, 2014.
- Morcinkowski B. *Simulative Analyse von zyklischen Schwankungen der kontrollierten ottomotorischen Selbstzündung*. PhD Dissertation, RWTH Aachen University, Aachen, 2015.
- Norouzi A, Ebrahimi K and Koch CR. Integral discrete-time sliding mode control of homogeneous charge compression ignition (HCCI) engine load and combustion timing. *IFAC-PapersOnline* 2019; 52(5): 153–158 (9th IFAC Symposium on Advances in Automotive Control AAC 2019), <http://www.sciencedirect.com/science/article/pii/S2405896319306445>.
- Nuss E, Wick M, Andert J, Schutter JD, Diehl M, Abel D, et al. Nonlinear model predictive control of a discrete-cycle gasoline-controlled auto ignition engine model: simulative analysis. *Int J Eng Res* 2019; 20(10): 1025–1036.
- Temel VK and Sterniak J. Characterization of SACI combustion for use in model based controls. SAE technical paper 2014-01-1289, 2014.
- Natarajan VK, Sick V, Reuss DL and Silvas G. Effect of spark-ignition on combustion periods during spark-assisted compression ignition. *Combust Sci Technol* 2009; 181(9): 1187–1206.
- Prakash N, Martz JB and Stefanopoulou AG. A phenomenological model for predicting the combustion phasing and variability of spark assisted compression ignition (SACI) engines. In: *ASME 2015 dynamic systems and control conference*, Columbus, OH, 28–30 October 2015. New York: ASME.
- Yıldız M and Çeper BA. Combustion development in a gasoline-fueled spark ignition-controlled auto-ignition engine operated at different spark timings and intake air temperatures. *Int J Eng Res*. Epub ahead of print 27 December 2019. DOI: 10.1177/1468087419894165.

24. Gordon D, Wouters C, Wick M, Xia F, Lehrheuer B, Andert J, et al. Development and experimental validation of a real-time capable FPGA based gas-exchange model for negative valve overlap. *Int J Eng Res* 2018; 21: 421–436.
25. Eng JA. Characterization of pressure waves in HCCI combustion. SAE technical paper 2002-01-2859, 2002.
26. Maurya RK. *Characteristics and control of low temperature combustion engines: employing gasoline, ethanol and methanol*. New York: Springer, 2017.
27. Hellström E, Stefanopoulou A, Vavra J, Babajimopoulos A, Assanis DN, Jiang L, et al. Understanding the dynamic evolution of cyclic variability at the operating limits of HCCI engines with negative valve overlap. *SAE Int J Eng* 2012; 5(3): 995–1008.
28. Gordon D, Wouters C, Wick M, Lehrheuer B, Andert J, Koch CR, et al. Development and experimental validation of a field programmable gate array-based in-cycle direct water injection control strategy for homogeneous charge compression ignition combustion stability. *Int J Eng Res* 2019; 20: 1101–1113.
29. Wouters C, Ottenwälder T, Lehrheuer B, Pischinger S, Wick M, Andert J, et al. Evaluation of the potential of direct water injection in HCCI combustion. SAE technical paper 2019-01-2165, 2019.
30. Wick M, Bedei J, Gordon D, Wouters C, Lehrheuer B, Nuss E, et al. In-cycle control for stabilization of homogeneous charge compression ignition combustion using direct water injection. *Appl Energ* 2019; 240: 1061–1074.
31. Thewes M, Baumgarten H, Scharf J, Birmes G, Balazs A, Lehrheuer B, et al. Water injection-high power and high efficiency combined. In: *25th Aachen colloquium automobile and engine technology*, Beijing, China, 9–11 November 2016, pp.345–380.
32. Hohenberg GF. Advanced approaches for heat transfer calculations. SAE technical paper 790825, 1979.